

Geometric response and disclination-induced skin effects in non-Hermitian systems

Xiao-Qi Sun,* Penghao Zhu,* and Taylor L. Hughes

Department of Physics and Institute for Condensed Matter Theory,
University of Illinois at Urbana-Champaign, Illinois 61801, USA

(Dated: February 28, 2025)

We study the geometric response of three-dimensional non-Hermitian crystalline systems with non-trivial point gap topology. For systems with four-fold rotation symmetry, we show that in presence of disclination lines with a total Frank angle which is an integer multiple of 2π , there can be non-trivial, one-dimensional point gap topology along the direction of disclination lines. This results in disclination-induced non-Hermitian skin effects. We extend the recently proposed non-Hermitian field theory approach to describe this phenomenon as a Euclidean Wen-Zee term. Furthermore, by doubling a non-Hermitian Hamiltonian to a Hermitian 3D chiral topological insulator, we show that the disclination-induced skin modes are zero modes of the surface Dirac fermion(s) in the presence of a pseudo-magnetic flux induced by disclinations.

Introduction.—Non-Hermitian Hamiltonians provide a natural formalism to describe wave phenomena in the presence of loss and gain, which are ubiquitous in a variety of physical contexts including condensed matter [1–4], photonic [5–17] and cold atom [18, 19] systems. Recently, there has been a growing interest in the interplay between non-Hermiticity and topological phases. The synergy of these two concepts has resulted in fruitful results that are distinct from Hermitian topological physics, such as new transport and dynamical features [20–27], new forms of bulk-boundary correspondence [28–35], and non-Hermitian analogy of topological insulators [36–44] and semimetals [45–60].

One of the most remarkable consequences of non-Hermiticity is new types of topological phases without Hermitian analogs. These intrinsically non-Hermitian topological phases are defined in the presence of a point gap with respect to a reference energy in the complex energy plane [61–68]. In one spatial dimension, the non-trivial point gap topology produces the celebrated non-Hermitian skin effect (NHSE) [31, 69–76], which generates an extensive number of states localized at the boundaries of a system. Recently, a topological field theory has been proposed which describes the response of non-Hermitian systems having non-trivial point gap topology to external gauge fields [77]. This approach led to a field theoretic description of the magnetic field induced NHSE in three-dimensional (3D) non-Hermitian Weyl semimetals with non-trivial point-gap topology [78]. In addition to electromagnetic response, there have been extensive studies of the *geometric* response of Hermitian topological systems both in the continuum limit [79–88] and at lattice level [89–97]. However, the understanding of the interplay between geometry and non-Hermitian point-gap topology is still preliminary.

In this letter, we consider the geometric response of 3D non-Hermitian crystalline systems having non-trivial point gap topology. We show that disclination lines in rotationally invariant systems can support 1D point gap topology along the direction of the disclination lines,

hence leading to a corresponding NHSE. In addition to our microscopic calculations, we show that we can describe this phenomenon with the inclusion of a Wen-Zee term [80] in the non-Hermitian field theory approach. Furthermore, by mapping the non-Hermitian problem to a 3D chiral topological insulator, we show that the disclination skin modes are zero modes of the surface Dirac fermions subjected to a pseudo-magnetic field induced by the disclinations.

Topological response.— 3D non-Hermitian crystalline systems can have a non-trivial point gap topology characterized by the point gap winding number $W_3(E)$ that is defined with respect to a reference energy E as [77, 78]:

$$W_3(E) = - \int_{\text{BZ}} \frac{d^3 k}{24\pi^3} \epsilon^{ijk} \text{tr} \left[(\tilde{H}^{-1} \partial_{k_i} \tilde{H}) \times (\tilde{H}^{-1} \partial_{k_j} \tilde{H}) (\tilde{H}^{-1} \partial_{k_k} \tilde{H}) \right], \quad (1)$$

where $\tilde{H}(\mathbf{k}) \equiv H(\mathbf{k}) - \mathbf{1}E$, and $H(\mathbf{k})$ is the non-Hermitian Bloch Hamiltonian. Non-Hermitian Hamiltonians with non-vanishing $W_3(E)$ exhibit a chiral magnetic skin effect, i.e., a NHSE along the direction of an applied magnetic field. This response is captured by a Euclidean topological field theory [77]:

$$S_E = \frac{W_3(E)}{4\pi} \int d^3 \mathbf{x} \epsilon^{ijk} A_i \partial_j A_k + \dots, \quad (2)$$

where we have written down the topological Chern-Simons term in the gradient expansion of the spatial vector potential $\mathbf{A}(\mathbf{x})$. From this action, the current response is $\mathbf{j} = \frac{W_3(E)}{2\pi} \mathbf{B}$, where the external magnetic field $\mathbf{B} = \nabla \times \mathbf{A}$.

To illustrate this effect consider $\mathbf{B} = B\hat{\mathbf{z}}$. We can choose a gauge that preserves translation symmetry along z , and then define a 1D point gap winding number $W_1(E)$ that captures the NHSE along the z -direction [63, 65, 77, 78]:

$$W_1(E) = - \int_0^{2\pi} \frac{dk_z}{2\pi} \frac{\partial}{\partial k_z} \arg [\det (H(\mathbf{A}, k_z) - E\mathbf{1})]. \quad (3)$$

It has been shown [77, 78] that the chiral current response is related to this 1D winding number, and hence the NHSE in the z -direction, through

$$W_1(E) = I_z = \int_S j_z dx dy = \frac{W_3}{2\pi} \int_S B_z dx dy, \quad (4)$$

where S is a surface at a fixed value of z . We note that the quantization of $W_1(E)$ is guaranteed for compact manifolds where the total magnetic flux along the z -direction is quantized.

Inspired by this formalism, we study the response of non-Hermitian systems with non-trivial W_3 to defects of the background geometry, which, as we will see, can effectively produce a pseudo-magnetic flux. From field-theory intuition of Hermitian systems, we can tentatively consider the effects predicted by a Euclidean Wen-Zee geometric response action [80, 98]:

$$S_{WZ} = \frac{\mathcal{L}_z W_3(E)}{2\pi} \int d^3 \mathbf{x} \epsilon^{ijk} A_i \partial_j \omega_k, \quad (5)$$

where ω is the spin connection that we treat as an effective gauge field, and \mathcal{L}_z is an orbital angular momentum. In exact analogy to Eq. (2) we can calculate the 1D point gap winding number induced by a flux of the spin-connection along the z -direction as

$$W_1(E) = I_z = \int_S j_z dx dy = \frac{\mathcal{L}_z W_3(E)}{2\pi} \int_S \Omega_z dx dy, \quad (6)$$

where $\Omega_z \equiv \partial_x \omega_y - \partial_y \omega_x$, and $W_1 > 0$ ($W_1 < 0$) indicates a NHSE with skin modes on the top (bottom) surface. To observe this effect we will generate the flux Ω_z by inserting disclinations in a lattice, which are represented by the Frank-angle vector $\Theta_i \equiv \int \Omega_i dS_i$ [90, 91, 94, 99]. We note that we have not derived Eq. (5), but instead proposed it to use as a guide to understand disclination-induced phenomena in concrete lattice models with C_{4z} rotation symmetry. This is because though treating disclinations as a pseudo-magnetic field has been studied extensively in the literature of disclinations [89, 93, 99–101], it can have subtleties due to the lattice regularization. We will see below that in certain cases the response of a lattice Hamiltonian to disclinations can be captured by Eq. (5), and we will clarify the deviation for the other cases.

Hermitian description.— In order to bridge the low energy effective theory discussed above with the NHSE observed in lattice models, it is convenient to introduce a doubled and Hermitianized Hamiltonian with chiral symmetry [63, 66]:

$$\mathcal{H}(\mathbf{k}) = \begin{pmatrix} 0 & H(\mathbf{k})^\dagger - E^* \\ H(\mathbf{k}) - E & 0 \end{pmatrix}, \quad (7)$$

where $H(\mathbf{k})$ is the non-Hermitian Hamiltonian we want to study, and E is the reference energy on which we focus. Two main features of this approach are: (i) the topological winding number $W_3(E)$ of $H(\mathbf{k})$ equals the chiral

winding number of $\mathcal{H}(\mathbf{k})$. Hence, the bulk-boundary correspondence of chiral symmetric insulators indicates that a nonzero $W_3(E)$ implies the existence of $|W_3(E)|$ protected surface Dirac cones (SDCs), and (ii) the existence of an *exact* zero mode of \mathcal{H} implies the existence of an eigenstate at energy E (E^*) for H (H^\dagger) depending on its chirality.

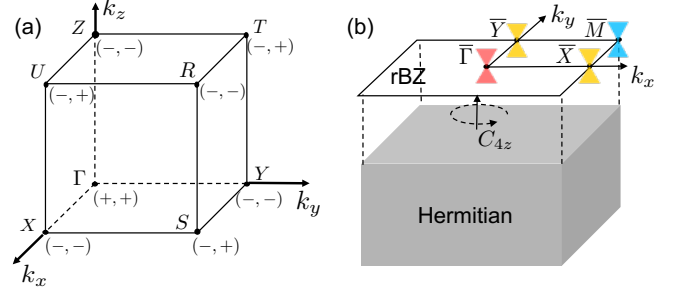


FIG. 1. (a) A tabulation of $(\text{sgn}[\gamma - \text{Im}E], \chi_i)$ at the eight Weyl points of Eq. (8) when $1 < \text{Im}E < 3$. (b) the locations of Dirac cone(s) on the surface of the Hermitian Hamiltonian in Eq. (7) when $1 < \text{Im}E < 3$ (red), $-1 < \text{Im}E < 1$ (yellow), and $-3 < \text{Im}E < -1$ (blue).

For an explicit illustration, let us focus on a concrete non-Hermitian Weyl semimetal model with a Bloch Hamiltonian:

$$H(\mathbf{k}) = t \sin k_x \sigma_x + t \sin k_y \sigma_y + t \sin k_z \sigma_z + i\gamma(\mathbf{k}), \quad (8)$$

where $\gamma(\mathbf{k}) = \cos k_x + \cos k_y + \cos k_z$. This model has a the C_{4z} rotational symmetry represented by:

$$C_{4z} = e^{-i\frac{\pi}{4}\sigma_z} e^{-i\pi\mathcal{L}_z/2}, \quad (9)$$

$$C_{4z} H(k_x, k_y, k_z) C_{4z}^\dagger = H(k_y, -k_x, k_z),$$

where the Pauli matrices represent the spin degree of freedom, and \mathcal{L}_z is the orbital angular momentum that takes values $-1, 0, 1, 2 \pmod{4}$, for C_{4z} symmetric systems. We will see below that the orbital rotation phase in Eq. (9) is important for the geometric response. For this model, the 3D winding number $W_3(E)$ has a simplified formula [78]:

$$W_3(E) = \sum_i \frac{1}{2} \text{sgn} [\gamma(\mathbf{Q}_i) - \text{Im}E] \chi_i, \quad (10)$$

where \mathbf{Q}_i are the momenta of the eight Weyl points in the Hermitian limit, and $\chi_i = \pm 1$ are their corresponding chiralities. The positions of the Weyl points in momentum space are shown in Fig. 1 (a), as well as their corresponding $(\text{sgn}[\gamma - \text{Im}E], \chi_i)$. This model therefore has a nontrivial 3D point gap winding number $W_3(E) = 1$ for $1 < |\text{Im}E| < 3$, and $W_3(E) = -2$ for $|\text{Im}E| < 1$.

Now we consider (the Hermitian) \mathcal{H} in a semi-infinite bulk geometry terminated with a surface normal \hat{z} and its 2D reduced Brillouin zone (rBZ) (see Fig. 1(b)). We start with the simple case where $1 < \text{Im}E < 3$ and

$W_3(E) = 1$. The low-energy effective Hamiltonian on the top C_{4z} -symmetric surface termination is a rotationally symmetric SDC at $\bar{\Gamma}$ as shown in Fig. 1(b) :

$$\mathcal{H}_{\text{eff}} = v(k_x \tau_x + k_y \tau_y), \quad (11)$$

where the Pauli matrices τ_i are the effective degrees of freedom, and the chiral symmetry is represented by τ_z .

Now we introduce disclination lines parallel to the z -direction. In addition to the coupling to τ_z , the spin connection also couples to $\mathcal{L}_z \mathbb{1}$, which adds an effective gauge flux $\mathcal{L}_z \Theta_z$ to a Dirac fermion affected by the disclination curvature sources [98]. According to the index theorem [102], this flux $\mathcal{L}_z \Theta_z$, will lead to robust zero modes on the top surface with total number $\nu = |\mathcal{L}_z \Theta_z/(2\pi)|$, assuming a continuous ω -field. Furthermore, the zero modes are eigenmodes of τ_z with eigenvalue (chirality) $\tau = \text{sgn } \mathcal{L}_z \Theta_z$ [98]. For $\mathcal{L}_z \Theta_z > 0$, the eigenmodes will have $\tau = +1$ and correspond to skin modes of H on the top surface and at energy E . By a similar argument for the bottom surface, one can derive that for $\mathcal{L}_z \Theta_z < 0$, there are zero modes of \mathcal{H} corresponding to skin modes of H on the bottom surface and at energy E . It is known [63] that the number of zero modes of \mathcal{H} with $\tau = +1$ equals $|W_1(E)|$, and that $\text{sgn}[W_1(E)] = +/-$ indicates that the zero modes with $\tau = +1$ are on the top/bottom surface. Hence, we can conclude that when $1 < \text{Im } E < 3$ and $W_3(E) = 1$, the disclination induces a winding number $W_1(E) = \mathcal{L}_z \Theta_z/(2\pi)$, which is fully captured by the Wen-Zee term in Eq. (5). We note that the effective flux is contributed *only* by the orbital rotation generator, which commutes with τ_i . From here on, we focus only on this part to compute the effective flux for a Dirac fermion in order to determine $W_1(E)$.

Let us proceed to discuss cases where the SDCs are at momenta away from $\bar{\Gamma}$. Since disclinations are classified by a Frank angle Θ_z and a Burgers vector (equivalence class) $\mathbf{b} = (b_x, b_y)$ [90, 91, 94], for a SDC with non-zero momentum, the Burgers vector will also contribute an effective flux of $-\mathbf{Q}_\perp \cdot \mathbf{b}$, which cannot be captured by the Wen-Zee action [103]. With this consideration in mind, let us analyze other topologically non-trivial regimes of our model. First, when $-3 < \text{Im } E < -1$, there is a single SDC at \bar{M} [see Fig. 1 (b)], and the effective flux it feels is [98]

$$\Phi^{\text{eff}}(\bar{M}) = \mathcal{L}_z \Theta_z - (\pi, \pi) \cdot \mathbf{b}. \quad (12)$$

From the index theorem for 2D Dirac fermions, and the relation between W_1 and the number of surface zero modes, it is straightforward to see that the effective flux in Eq.(12) leads to a winding number $W_1(E) = \Phi^{\text{eff}}(\bar{M})/(2\pi)$. Second, when $-1 < \text{Im } E < 1$, there is a pair of SDCs at \bar{X} and \bar{Y} [see Fig. 1 (b)]. Since a C_{4z} rotation takes one SDC to another, and the translation phase obtained by each SDC is different, these two SDCs together form an irreducible representation of the space

group. A subtlety arises that we cannot *individually* define the effective flux for each SDC, and need to consider the (possibly *non-Abelian*) effective flux of both. In doing so, we write the C_{4z} rotation operator for these two SDCs acting on *orbital* degrees of freedom:

$$C_{4z} = \sigma_x^v e^{-i\frac{\pi}{2}\mathcal{L}_z} = \exp\left(-i\frac{\pi}{2}\mathcal{L}_z \sigma_x^v\right), \quad (13)$$

where the superscript v indicates the operator is in the valley space, and σ_x^v exchanges the two valleys \bar{X} and \bar{Y} . From Eq.(13), we can see $\mathcal{L}_z \sigma_x^v$ is the orbital rotation generator, which leads to a non-Abelian flux for SDCs at the two valleys. The effective flux can be written as $\Phi_r = \mathcal{L}_z \Theta_z \sigma_x^v$, where Θ_z is a multiple of $\pi/2$ in the C_{4z} -symmetric case. In addition, the translation phase of SDCs at the two valleys contributes another matrix flux:

$$\Phi_t = -\pi \begin{pmatrix} b_x & 0 \\ 0 & b_y \end{pmatrix}. \quad (14)$$

Combining these two contributions, we define the total non-Abelian effective flux felt by SDCs at two valleys to be

$$e^{i\Phi^{\text{eff}}(\bar{X}\bar{Y})} = e^{i\Phi_t} e^{i\Phi_r}. \quad (15)$$

Now applying the index theorem again [98], we find a winding number $W_1(E) = -\text{tr}[\Phi^{\text{eff}}(\bar{X}\bar{Y})]/(2\pi)$, where the minus sign comes from the chiral winding number -1 of the SDCs. Notice that the analysis from the index theorem is in continuum limit, however, we will show that this indeed captures the disclination-induced skin effect in our lattice model [c.f. Eq.(8)].

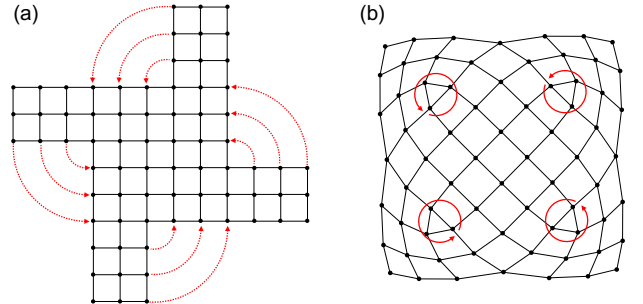


FIG. 2. Schematic illustration of a lattice construction with four disclinations, each of which has Frank angle $-\pi/2$. (a) is the gluing procedure [98], and (b) is a completed lattice with disclinations.

Numerical results.— To find a quantized $W_1(E)$ and the corresponding NHSE, we need a total pseudo-magnetic (time-reversal odd) flux that is an integer multiple of 2π . However, there is a subtlety on the lattice that a flux of $n\pi$ passing through a single lattice plaquette is time-reversal invariant and incompatible with a chiral current I_z response and the corresponding NHSE [c.f. Eq.(6)]. Thus, for our lattice calculations this motivates us to consider orbital angular momentum $\mathcal{L}_z = \pm 1$, and introduce

four disclinations each with Frank angle $\Theta_z^s = \pm\pi/2$, where the superscript s is to distinguish the Frank angle of a *single* disclination and the total Frank angle Θ_z in the system. For illustration purposes, let us fix $\mathcal{L}_z = 1$, and focus on the case where each of the four disclinations has a Frank angle $\Theta_z^s = -\pi/2$ in the following. We discuss other cases, e.g., $(\Theta_z^s = -\pi/2, \mathcal{L}_z = -1)$, and $(\Theta_z^s = \pi/2, \mathcal{L}_z = +1)$, etc., in the Supplemental Material [98].

For our lattice calculations we construct four disclinations with Frank angle $\Theta_z^s = -\pi/2$ by a process shown in Fig. 2 [98]. Then, we add the hopping terms determined by the Hamiltonian in Eq. (8) on the disclinated lattice to derive a Hamiltonian $H_{\text{dis}}(k_z)$. We note that we are using disclinations with “plaquette-type” cores [90] which implies a Burgers vector *class* $\mathbf{b}^s = a\hat{x}$, where a is the lattice constant and the superscript s indicates the Burgers vector is for a *single* disclination. Note that because of the C_{4z} symmetry we could equivalently say that $\mathbf{b}^s = a\hat{y}$, hence a Burgers vector class. Let us first focus on the simplest regime when $1 < \text{Im } E < 3$ and $W_3(E) = 1$. To show the nontrivial 1D point gap winding number $W_1(E) = -1$ [c.f. Eq.(3)] of $H_{\text{dis}}(k_z)$, we plot $\arg \det(H_{\text{dis}}(k_z) - E\mathbb{1})$ at $E = 2i$ in Fig. 3 (a). Fig. 3 (b) shows the spectrum of H_{dis} under periodic boundary conditions along the z -direction, where a loop circling the $1 < \text{Im } E < 3$ region can be seen. The skin modes on the *bottom* surface, which are qualitatively captured by $W_1(E) = -1$, are indicated by blue dots in Fig. 3 (c) which is the spectrum with open boundary conditions in the z -direction. We find ten skin modes in the region $1 < \text{Im } E < 3$, which is consistent with the extensive NHSE for a 1D line in a 3D system where $N_z = 10$. In Fig. 3 (d) we show an exponentially decaying wavefunction of a representative skin mode (circled in Fig. 3 (c)). Hence, when $1 < \text{Im } E < 3$, $\mathcal{L}_z = +1$, and there is pseudo-magnetic flux -2π , we have shown numerically that $W_1(E) = -1$ and there are corresponding skin modes, which is consistent with the Wen-Zee term [c.f. Eq. (5)] and our Hermitian understanding above [104].

Next, consider the regime when $-3 < \text{Im } E < -1$. Since each of the four disclinations in Fig. 2 have Burgers vector class $\mathbf{b}^s = a\hat{x}$, the effective flux [c.f. Eq. (12)] contributed from each disclination is $-3\pi/2$, which is equivalent to $\pi/2$. In total, there is a $\Phi^{\text{eff}}(\bar{M}) = 2\pi$ pseudo-magnetic flux, and we expect a nontrivial 1D point gap winding, $W_1(E) = +1$, which is confirmed by our numerical calculation shown in Fig. 4 (a). Finally, consider the regime when $-1 < \text{Im } E < 1$. By substituting $\mathbf{b}^s = a\hat{x}$ and $\Omega_z = -\pi/2$ into Φ_t and Φ_r defined above, one can calculate $e^{i\Phi^{\text{eff}}(\bar{X}\bar{Y})} = \sigma_y^v$, of which the two eigenmodes feel time-reversal invariant flux ($\Phi_1 = 0$ and $\Phi_2 = \pi$) on each disclination, and thus we expect a trivial 1D point gap winding $W_1(E) = 0$. This is confirmed by our numerical calculation shown in Fig. 4(b).

Conclusions.—We studied the geometric response of

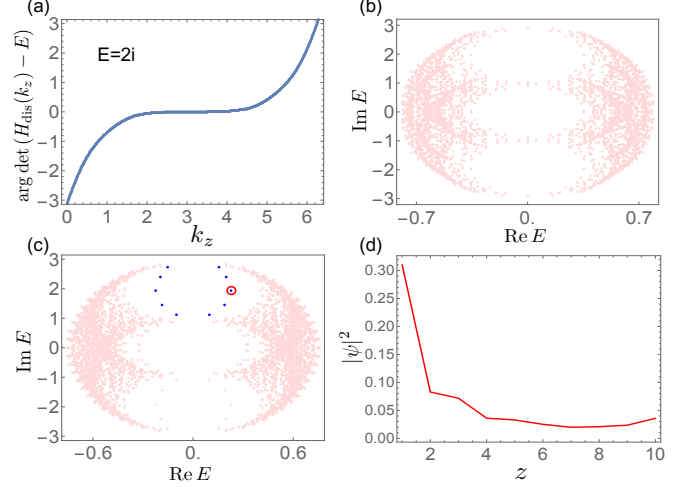


FIG. 3. Numerical calculations for the non-Hermitian Weyl semimetal described by Eq. (8) on a lattice with four disclinations as shown in Fig. 2, and $t = 1/2$ is used in all calculations. The lattice has 10 unit cells along z -direction, and 200 unit cells in the x - y plane at each z . (a) shows the nontrivial one-dimensional point gap winding number $W_1(E)$ at $E = 2i$. (b) and (c) show the energy spectrum under periodic and open boundary condition along z , where the blue dots in (c) are skin modes on the bottom surface. (d) shows the wave-function along z direction for the state indicated by a red circle in (c).

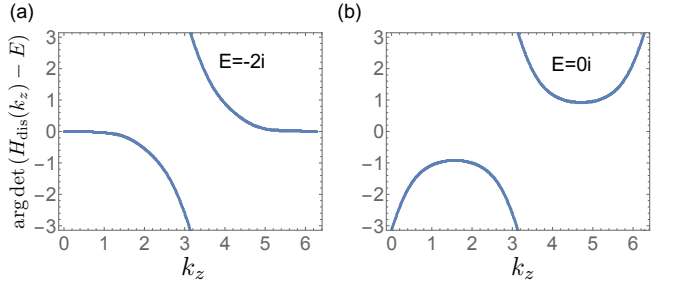


FIG. 4. The 1D point gap winding number $W_1(E)$ on a lattice with four disclinations as shown in Fig. 2 for (a) $E = -2i$ and (b) $E = 0i$.

a C_{4z} -symmetric 3D non-Hermitian lattice model with non-trivial point-gap topology characterized by W_3 . We find that disclinations can induce NHSEs along the disclination lines. We compared our explicit lattice calculations with a proposed Euclidean Wen-Zee term in an effective non-Hermitian response field theory. Interestingly, we found that for the case where the SDC of the Hermitianized Hamiltonian is located at the $\bar{\Gamma}$ point, the Wen-Zee action predicted the correct 1D winding number W_1 , while in other cases one must consider a combination of rotation and translation lattice information for the low energy theory to properly explain the resulting 1D winding number and existence/non-existence of the NHSE. In the future, we expect that our model can be realized in various platforms, including photonic, mechanical, and

circuit systems [70–75]. Furthermore, our model study serves as a first concrete example to understand geometric response in non-Hermitian topological phases and will motivate future theoretical endeavors in this direction.

Acknowledgments.— X.-Q. S. acknowledges support from the Gordon and Betty Moore Foundations EPiQS Initiative through Grant GBMF8691. P. Z. and T. L. H. thank the US Office of Naval Research (ONR) Multi-disciplinary University Research Initiative (MURI) grant N00014-20- 1-2325 on Robust Photonic Materials with High-Order Topological Protection for support.

* These two authors contributed equally.

- [1] V. Kozii and L. Fu, [arXiv:1708.05841](#) (2017).
- [2] H. Shen and L. Fu, *Phys. Rev. Lett.* **121**, 026403 (2018).
- [3] M. Papaj, H. Isobe, and L. Fu, [arXiv:1802.00443](#) (2018).
- [4] A. A. Zyuzin and A. Y. Zyuzin, *Phys. Rev. B* **97**, 041203 (2018).
- [5] H. Schomerus, *Opt. Lett.* **38**, 1912 (2013).
- [6] B. Zhen, C. W. Hsu, Y. Igarashi, L. Lu, I. Kaminer, A. Pick, S.-L. Chua, J. D. Joannopoulos, and M. Soljačić, *Nature* **525**, 354 (2015).
- [7] J. M. Zeuner, M. C. Rechtsman, Y. Plotnik, Y. Lumer, S. Nolte, M. S. Rudner, M. Segev, and A. Szameit, *Phys. Rev. Lett.* **115**, 040402 (2015).
- [8] L. Lu, Z. Wang, D. Ye, L. Ran, L. Fu, J. D. Joannopoulos, and M. Soljačić, *Science* **349**, 622 (2015).
- [9] C. Poli, M. Bellec, U. Kuhl, F. Mortessagne, and H. Schomerus, *Nat. Comm.* **6**, 6710 (2015).
- [10] S. Weimann, M. Kremer, Y. Plotnik, Y. Lumer, S. Nolte, K. G. Makris, M. Segev, M. C. Rechtsman, and A. Szameit, *Nat. Mater.* **16**, 433 (2016).
- [11] W.-J. Chen, M. Xiao, and C. T. Chan, *Nat. Comm.* **7**, 13038 (2016).
- [12] J. Noh, S. Huang, D. Leykam, Y. D. Chong, K. P. Chen, and M. C. Rechtsman, *Nat. Phys.* **13**, 611 (2017).
- [13] L. Xiao, X. Zhan, Z. H. Bian, K. K. Wang, X. Zhang, X. P. Wang, J. Li, K. Mochizuki, D. Kim, N. Kawakami, W. Yi, H. Obuse, B. C. Sanders, and P. Xue, *Nat. Phys.* **13**, 1117 (2017).
- [14] X. Zhan, L. Xiao, Z. Bian, K. Wang, X. Qiu, B. C. Sanders, W. Yi, and P. Xue, *Phys. Rev. Lett.* **119**, 130501 (2017).
- [15] K. Takata and M. Notomi, *Phys. Rev. Lett.* **121**, 213902 (2018).
- [16] H. Zhou, C. Peng, Y. Yoon, C. W. Hsu, K. A. Nelson, L. Fu, J. D. Joannopoulos, M. Soljačić, and B. Zhen, *Science* **359**, 1009 (2018).
- [17] A. Cerjan, S. Huang, M. Wang, K. P. Chen, Y. Chong, and M. C. Rechtsman, *Nature Photonics* **13**, 623 (2019).
- [18] Y. Choi, S. Kang, S. Lim, W. Kim, J.-R. Kim, J.-H. Lee, and K. An, *Phys. Rev. Lett.* **104**, 153601 (2010).
- [19] Y. Xu, S.-T. Wang, and L.-M. Duan, *Phys. Rev. Lett.* **118**, 045701 (2017).
- [20] M. S. Rudner and L. S. Levitov, *Phys. Rev. Lett.* **102**, 065703 (2009).
- [21] A. McDonald, T. Pereg-Barnea, and A. A. Clerk, *Phys. Rev. X* **8**, 041031 (2018).
- [22] F. Song, S. Yao, and Z. Wang, *Phys. Rev. Lett.* **123**, 170401 (2019).
- [23] J. Y. Lee, J. Ahn, H. Zhou, and A. Vishwanath, *Phys. Rev. Lett.* **123**, 206404 (2019).
- [24] C. C. Wanjura, M. Brunelli, and A. Nunnenkamp, *Nature communications* **11**, 1 (2020).
- [25] W.-T. Xue, M.-R. Li, Y.-M. Hu, F. Song, and Z. Wang, [arXiv preprint arXiv:2004.09529](#) (2020).
- [26] L. Li, S. Mu, and J. Gong, [arXiv preprint arXiv:2012.08799](#) (2020).
- [27] H. Schomerus, *Phys. Rev. Research* **2**, 013058 (2020).
- [28] T. E. Lee, *Phys. Rev. Lett.* **116**, 133903 (2016).
- [29] D. Leykam, K. Y. Bliokh, C. Huang, Y. D. Chong, and F. Nori, *Phys. Rev. Lett.* **118**, 040401 (2017).
- [30] S. Yao, F. Song, and Z. Wang, *Phys. Rev. Lett.* **121**, 136802 (2018).
- [31] S. Yao and Z. Wang, *Phys. Rev. Lett.* **121**, 086803 (2018).
- [32] F. K. Kunst, E. Edvardsson, J. C. Budich, and E. J. Bergholtz, *Phys. Rev. Lett.* **121**, 026808 (2018).
- [33] C. H. Lee, G. Li, Y. Liu, T. Tai, R. Thomale, and X. Zhang, [arXiv:1812.02011](#) (2018).
- [34] K. Yokomizo and S. Murakami, *Phys. Rev. Lett.* **123**, 066404 (2019).
- [35] H.-G. Zirnstein, G. Refael, and B. Rosenow, [arXiv:1901.11241](#) (2019).
- [36] Z. Gong, Y. Ashida, K. Kawabata, K. Takasan, S. Higashikawa, and M. Ueda, *Phys. Rev. X* **8**, 031079 (2018).
- [37] H. Zhou and J. Y. Lee, *Phys. Rev. B* **99**, 235112 (2019).
- [38] T. Liu, Y.-R. Zhang, Q. Ai, Z. Gong, K. Kawabata, M. Ueda, and F. Nori, *Phys. Rev. Lett.* **122**, 076801 (2019).
- [39] K. Kawabata, K. Shiozaki, M. Ueda, and M. Sato, *Phys. Rev. X* **9**, 041015 (2019).
- [40] M. R. Hirsbrunner, T. M. Philip, and M. J. Gilbert, *Phys. Rev. B* **100**, 081104 (2019).
- [41] W. Xi, Z.-H. Zhang, Z.-C. Gu, and W.-Q. Chen, [arXiv preprint arXiv:1911.01590](#) (2019).
- [42] C. C. Wojcik, X.-Q. Sun, T. Bzdušek, and S. Fan, *Phys. Rev. B* **101**, 205417 (2020).
- [43] M. M. Denner, A. Skurativska, F. Schindler, M. H. Fischer, R. Thomale, T. Bzdušek, and T. Neupert, [arXiv preprint arXiv:2008.01090](#) (2020).
- [44] Y. Ma and T. L. Hughes, [arXiv preprint arXiv:2008.02284](#) (2020).
- [45] A. Cerjan, M. Xiao, L. Yuan, and S. Fan, *Phys. Rev. B* **97**, 075128 (2018).
- [46] Q. Zhong, M. Khajavikhan, D. N. Christodoulides, and R. El-Ganainy, *Nature Communications* **9**, 4808 (2018).
- [47] V. M. Martinez Alvarez, J. E. Barrios Vargas, and L. E. F. Foa Torres, *Phys. Rev. B* **97**, 121401 (2018).
- [48] J. Carlström and E. J. Bergholtz, *Phys. Rev. A* **98**, 042114 (2018).
- [49] R. Okugawa and T. Yokoyama, *Phys. Rev. B* **99**, 041202 (2019).
- [50] J. Carlström, M. Stålhammar, J. C. Budich, and E. J. Bergholtz, *Phys. Rev. B* **99**, 161115 (2019).
- [51] K. Moors, A. A. Zyuzin, A. Y. Zyuzin, R. P. Tiwari, and T. L. Schmidt, *Phys. Rev. B* **99**, 041116 (2019).
- [52] T. Yoshida, R. Peters, N. Kawakami, and Y. Hatsugai, *Phys. Rev. B* **99**, 121101 (2019).
- [53] P. A. McClarty and J. G. Rau, *Phys. Rev. B* **100**, 100405 (2019).

[54] K. Kawabata, T. Bessho, and M. Sato, *Phys. Rev. Lett.* **123**, 066405 (2019).

[55] E. J. Bergholtz, J. C. Budich, and F. K. Kunst, *arXiv:1912.10048* (2019).

[56] J. C. Budich, J. Carlström, F. K. Kunst, and E. J. Bergholtz, *Phys. Rev. B* **99**, 041406 (2019).

[57] Z. Yang and J. Hu, *Phys. Rev. B* **99**, 081102 (2019).

[58] H. Wang, J. Ruan, and H. Zhang, *Phys. Rev. B* **99**, 075130 (2019).

[59] T. Yoshida, R. Peters, N. Kawakami, and Y. Hatsugai, *arXiv:2002.11265* (2020).

[60] X.-Q. Sun, C. C. Wojcik, S. Fan, and T. Bzdušek, *Phys. Rev. Research* **2**, 023226 (2020).

[61] C. H. Lee and R. Thomale, *Phys. Rev. B* **99**, 201103 (2019).

[62] C. H. Lee, L. Li, and J. Gong, *Phys. Rev. Lett.* **123**, 016805 (2019).

[63] N. Okuma, K. Kawabata, K. Shiozaki, and M. Sato, *Phys. Rev. Lett.* **124**, 086801 (2020).

[64] D. S. Borgnia, A. J. Kruchkov, and R.-J. Slager, *Phys. Rev. Lett.* **124**, 056802 (2020).

[65] K. Zhang, Z. Yang, and C. Fang, *Phys. Rev. Lett.* **125**, 126402 (2020).

[66] K. Kawabata, M. Sato, and K. Shiozaki, *Phys. Rev. B* **102**, 205118 (2020).

[67] R. Okugawa, R. Takahashi, and K. Yokomizo, *Phys. Rev. B* **102**, 241202 (2020).

[68] Y. Fu, J. Hu, and S. Wan, *Phys. Rev. B* **103**, 045420 (2021).

[69] N. Hatano and D. R. Nelson, *Phys. Rev. Lett.* **77**, 570 (1996).

[70] S. Longhi, D. Gatti, and G. Della Valle, *Scientific reports* **5**, 1 (2015).

[71] A. Ghatak, M. Brandenbourger, J. van Wezel, and C. Coulais, *Proceedings of the National Academy of Sciences* **117**, 29561 (2020).

[72] L. Xiao, T. Deng, K. Wang, G. Zhu, Z. Wang, W. Yi, and P. Xue, *Nature Physics* , 1 (2020).

[73] S. Weidemann, M. Kremer, T. Helbig, T. Hofmann, A. Stegmaier, M. Greiter, R. Thomale, and A. Szameit, *Science* **368**, 311 (2020).

[74] T. Helbig, T. Hofmann, S. Imhof, M. Abdelghany, T. Kiessling, L. Molenkamp, C. Lee, A. Szameit, M. Greiter, and R. Thomale, *Nature Physics* **16**, 747 (2020).

[75] T. Hofmann, T. Helbig, F. Schindler, N. Salgo, M. Brzezińska, M. Greiter, T. Kiessling, D. Wolf, A. Vollhardt, A. Kabashi, C. H. Lee, A. Bilušić, R. Thomale, and T. Neupert, *Phys. Rev. Research* **2**, 023265 (2020).

[76] L. S. Palacios, S. Tchoumakov, M. Guix, I. Pagonabarraga, S. Sánchez, and A. G. Grushin, *arXiv:2012.14496* (2020).

[77] K. Kawabata, K. Shiozaki, and S. Ryu, *arXiv:2011.11449* (2020).

[78] T. Bessho and M. Sato, *arXiv:2006.04204* (2020).

[79] J. Avron, R. Seiler, and P. G. Zograf, *Physical review letters* **75**, 697 (1995).

[80] X. G. Wen and A. Zee, *Phys. Rev. Lett.* **69**, 953 (1992).

[81] N. Read, *Physical Review B* **79**, 045308 (2009).

[82] T. L. Hughes, R. G. Leigh, and E. Fradkin, *Physical review letters* **107**, 075502 (2011).

[83] B. Bradlyn, M. Goldstein, and N. Read, *Physical Review B* **86**, 245309 (2012).

[84] T. L. Hughes, R. G. Leigh, and O. Parrikar, *Phys. Rev. D* **88**, 025040 (2013).

[85] A. G. Abanov and A. Gromov, *Phys. Rev. B* **90**, 014435 (2014).

[86] A. Gromov and A. G. Abanov, *Phys. Rev. Lett.* **113**, 266802 (2014).

[87] A. Gromov, G. Y. Cho, Y. You, A. G. Abanov, and E. Fradkin, *Phys. Rev. Lett.* **114**, 016805 (2015).

[88] R. R. Biswas and D. T. Son, *Proceedings of the National Academy of Sciences* **113**, 8636 (2016).

[89] M. Vozmediano, M. Katsnelson, and F. Guinea, *Physics Reports* **496**, 109 (2010).

[90] J. C. Y. Teo and T. L. Hughes, *Phys. Rev. Lett.* **111**, 047006 (2013).

[91] W. A. Benalcazar, J. C. Y. Teo, and T. L. Hughes, *Phys. Rev. B* **89**, 224503 (2014).

[92] H. Shapourian, T. L. Hughes, and S. Ryu, *Phys. Rev. B* **92**, 165131 (2015).

[93] S. Liu, A. Vishwanath, and E. Khalfaf, *Phys. Rev. X* **9**, 031003 (2019).

[94] T. Li, P. Zhu, W. A. Benalcazar, and T. L. Hughes, *Phys. Rev. B* **101**, 115115 (2020).

[95] P. Rao and B. Bradlyn, *Phys. Rev. X* **10**, 021005 (2020).

[96] C. W. Peterson, T. Li, W. Jiang, T. L. Hughes, and G. Bahl, *Nature* **589**, 376 (2021).

[97] Y. Liu, S. Leung, F.-F. Li, Z.-K. Lin, X. Tao, Y. Poo, and J.-H. Jiang, *Nature* **589**, 381 (2021).

[98] See Supplemental Material at *missing URL!* for (i) detailed discussion of the effectiv flux and the index theorem, (ii) details of numerical calculations.

[99] B. Han, H. Wang, and P. Ye, *Phys. Rev. B* **99**, 205120 (2019).

[100] R. Thorngren and D. V. Else, *Phys. Rev. X* **8**, 011040 (2018).

[101] Y. You, T. Devakul, F. J. Burnell, and T. Neupert, *Phys. Rev. B* **98**, 235102 (2018).

[102] M. Nakahara, *Geometry, Topology and Physics* (Taylor & Francis Group, Abingdon, 2003).

[103] To be precise, we note that this translation phase can be represented in a response action as a coupling to gauge fields for the translation symmetry, which is represented frame fields e_μ^a . The justification of this effective flux and the response action can be found in the Supplemental Material [98].

[104] Numerical results for all other cases with $1 < \text{Im } E < 3$ (i.e., $\mathcal{L}_z = -1$ and pseudo-magnetic flux -2π , and $\mathcal{L}_z = \pm 1$ and pseudo-magnetic flux $+2\pi$) are shown in the Supplemental Material, and are also consistent with Eq. (5) and our Hermitian understanding.

SUPPLEMENTAL MATERIAL FOR: GEOMETRIC RESPONSE AND DISCLINATION-INDUCED SKIN EFFECTS IN NON-HERMITIAN SYSTEMS

EFFECTIVE FLUX FROM INDEX THEOREM

In this section, we justify the index theorem for SDCs used in the main text. In our case, we have rotation (around z -direction) generator $\mathcal{L}_z \mathbb{1} + \tau_z/2$ for a SDC (at $\bar{\Gamma}$). When the system is disclinated, the spin connection ω_μ with $\mu = 1, 2$ will enter the Dirac operator, which can be written as

$$\not{D}_{SDC} = e_a^\mu \gamma^a [\mathbb{1} \partial_\mu - i \omega_\mu (\mathcal{L}_z \mathbb{1} + \tau_z/2)] = e_a^\mu \gamma^a (\mathbb{1} \partial_\mu - i \mathcal{L}_z \omega_\mu \mathbb{1} - i \omega_\mu \tau_z/2), \quad (\text{S1})$$

where e_a^μ is the frame field and $\gamma^{1,2} = \tau_{x,y}$. If we compare Eq.(S1) with the most general Dirac operator coupled to a U(1) gauge field and to the background geometry:

$$\not{D} = e_a^\mu \gamma^a (\mathbb{1} \partial_\mu - i A_\mu \mathbb{1} - \frac{i}{4} \omega_\mu^{ab} \gamma_{ab}), \quad (\text{S2})$$

where ω_μ^{ab} is the spin connection, we can see ω_μ in Eq.(S1) is just a short form for $\omega_\mu^{12} = -\omega_\mu^{21}$, and correspondingly $\gamma^{12} = -\gamma^{21} = \tau_z$. If we further consider $\mathcal{L}_z \omega_\mu$ as an effective Abelian gauge field A_μ^{eff} , it is straightforward to see that Eq. (S1) is just a special case of Eq. (S2) on a manifold M described by the fixed ω_μ^{ab} . Then we can apply the index theorem for the general Dirac operator [see Chapter 12 of Ref. 102] to Eq. (S1):

$$\nu_+ - \nu_- = \frac{1}{2\pi} \int_M \partial_x A_y^{\text{eff}} - \partial_y A_x^{\text{eff}} = \frac{\mathcal{L}_z}{2\pi} \int_M \partial_x \omega_y - \partial_y \omega_x = \frac{\mathcal{L}_z \Theta_z}{2\pi}, \quad (\text{S3})$$

where ν_+ (ν_-) is the number of zero modes with chirality $\tau = +1$ (-1). There are a total of $\nu \equiv |\nu_+ - \nu_-|$ number of robust zero modes. In the case of $\nu_+ - \nu_- > 0$, the ν robust zero modes have chirality $\tau = +1$, which corresponds to skin modes. We note that the RHS of Eq.(S3) only has contribution from the flux of the (effective) abelian gauge field, and has no contribution from the coupling of spin connection to γ_{ab} , which is true for Dirac operators in 2D [102]. We also note that the above discussion is for a SDC with chiral winding number $+1$, for SDCs with chiral winding number -1 there will be an extra minus sign on the RHS of Eq.(S3). To apply the index theorem in the main text, we should consider that the top SDC has chiral winding number $\text{sgn}[W_3(E)]$ and the bottom SDC have the opposite chiral winding number in our model. With similar analysis, we can also find the effective Abelian/non-Abelian gauge flux and use the correct index theorem in other cases.

When the SDC at \bar{M} , we add an extra flux related to translation, $-(\pi, \pi) \cdot \mathbf{b}$, to the effective flux. This is because for SDCs with non-zero momenta $\mathbf{Q}_\perp = (Q_x, Q_y)$, there will be another effective gauge field $-Q_{\perp,a} e_\mu^a$ besides $\omega_\mu \mathcal{L}_z$ and the extra effective gauge flux can be computed as

$$-Q_{\perp,a} \oint dx^\mu e_\mu^a = -Q_{\perp,a} b^a = -\mathbf{Q}_\perp \cdot \mathbf{b}. \quad (\text{S4})$$

Like the effective flux from $\omega_\mu \mathcal{L}_z$ can be captured by a bulk Wen-Zee term in Eq. (5) of the main text, we tentatively propose a term at low energy to capture the translation phase:

$$S_t = \frac{1}{2\pi} \int d^3 \mathbf{x} \epsilon^{ijk} A_i Q_{\perp,a} \partial_j e_k^a, \quad (\text{S5})$$

the details of which will be left to future research.

When there are a pair of SDCs at X and Y of the same winding number, we have a 2D Dirac operator under a non-Abelian effective gauge field related to orbital angular momentum, $\mathcal{L}_z \sigma_x^v \otimes \mathbb{1}$, and a non-Abelian effective gauge field related to translation, $\begin{pmatrix} (\pi, 0) \cdot \mathbf{e}_\mu & 0 \\ 0 & (0, \pi) \cdot \mathbf{e}_\mu \end{pmatrix} \otimes \mathbb{1}$. Then, we need to consider the non-Abelian effective flux $\Phi^{\text{eff}}(\bar{X}\bar{Y})$ contributed by both and we have

$$\nu_+ - \nu_- = \pm \text{sgn}[W_3(E)] \frac{\text{tr} [\Phi^{\text{eff}}(\bar{X}\bar{Y})]}{2\pi}, \quad (\text{S6})$$

for the top/bottom surface as used in the main text.

SUPPLEMENTAL INFORMATION FOR NUMERICAL CALCULATIONS

Here, we first describe more details about how we perform the numerical calculations. When gluing the open edges at ϕ and $\phi + \pi/2$ shown in Fig. 2 (a) in the main text, we add a phase $\exp(-i\mathcal{L}_z\pi/2)$. This is because by rotating one edge anti-clockwisely by $\pi/2$ to glue it with another edge, the states on that edge will obtain a phase $\exp(-i\mathcal{L}_z\pi/2)$. Meanwhile, we also rotate σ_x to σ_y , and rotate σ_y to $-\sigma_x$ when gluing. This part is given by the rotation of the internal degrees of freedom (or spin), which is generated by σ_z .

Next, we present numerical results for $\mathcal{L}_z = \pm 1$ in the lattice where there are four disclinations, each of them has $\Theta_z^s = \pm\pi/2$. In summary, the main conclusions we can draw from these results are: (i) the 1D point gap winding number for the $1 < \text{Im } E < 3$ case can be correctly predicted by the Wen-Zee term in Eq. (5). However, (ii) the correct prediction of 1D point gap winding number for the $-3 < \text{Im } E < -1$ case and the $-1 < \text{Im } E < 1$ case requires a combination of rotation and translation lattice information, and can be done through including an extra effective flux as shown in the last section.

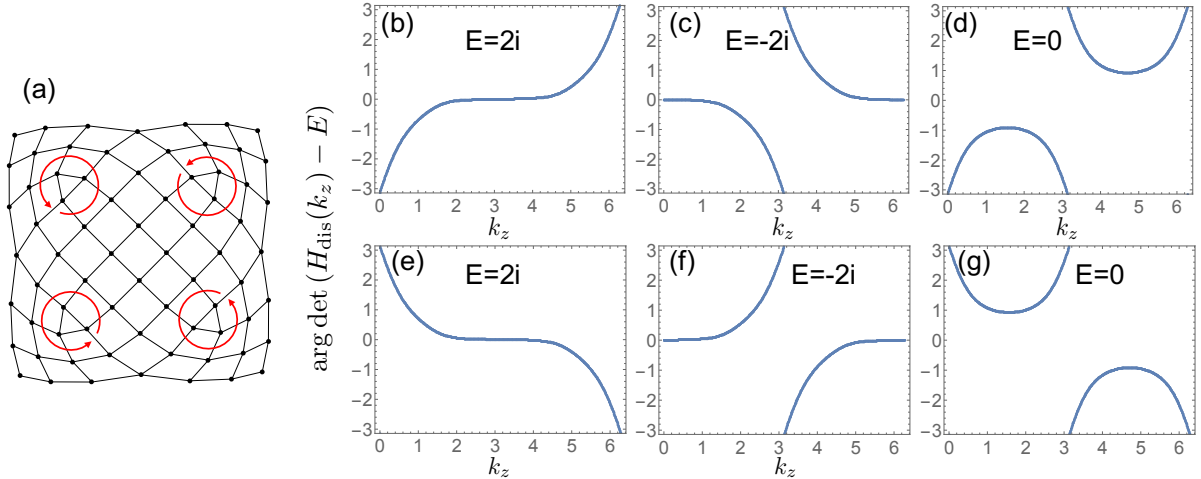


FIG. S1. Numerical calculations for a non-Hermitian Weyl semimetal described by Eq. (8) in a lattice where there are four disclinations with Frank angle $-\pi/2$ as shown in (a). (b), (c) and (d) are for $\mathcal{L}_z = 1$. (e), (f) and (g) are for $\mathcal{L}_z = -1$.

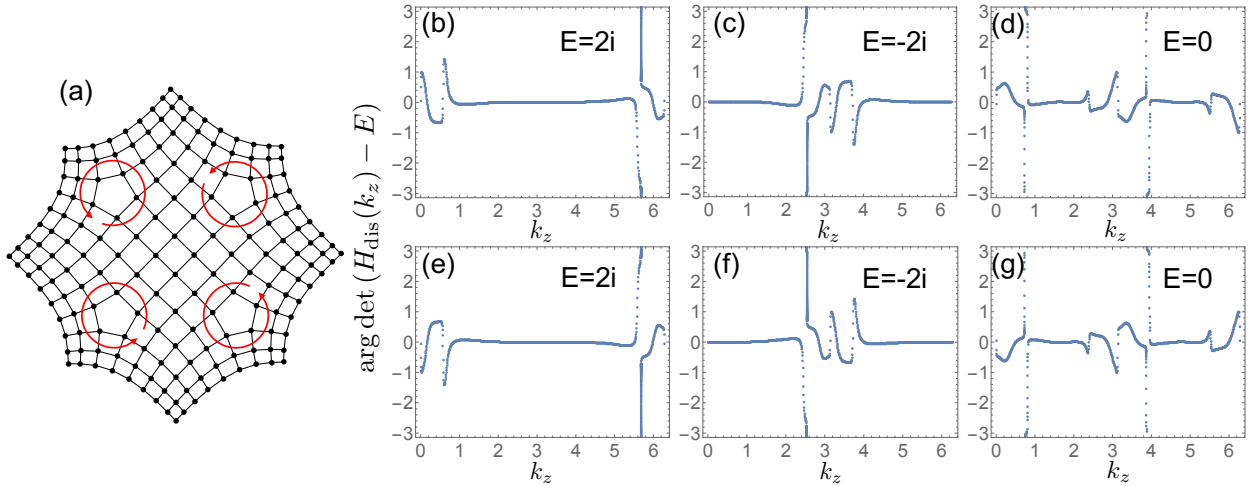


FIG. S2. Numerical calculations for a non-Hermitian Weyl semimetal described by Eq. (8) in a lattice where there are four disclinations with Frank angle $\pi/2$ as shown in (a). (b), (c) and (d) are for $\mathcal{L}_z = 1$. (e), (f) and (g) are for $\mathcal{L}_z = -1$.